

# 000 001 002 003 004 005 006 007 008 009 010 011 012 013 014 015 016 017 018 019 020 021 022 023 024 025 026 027 028 029 030 031 032 033 034 035 036 037 038 039 040 041 042 043 044 045 046 047 048 049 050 051 052 053 COMPLEMENTARITY MATTERS: A CLOSER LOOK AT NEAREST NEIGHBOR GUIDANCE FOR OOD DETEC- TION

Anonymous authors

Paper under double-blind review

## ABSTRACT

Out-of-distribution (OOD) detection seeks to identify inputs that fall outside the training distribution, which is crucial for ensuring the reliability of deep neural networks (DNNs). The dominant approach to OOD detection is score-based: each sample receives a score, and those with scores that differ significantly from the training data are flagged as out-of-distribution. The most effective score functions typically rely on DNN’s classifier uncertainty, or nearest-neighbour (NN) similarity of test and training samples. Moreover, recent research demonstrates that combining the classifier- and NN-based scores - the process called NN Guidance - yields the best OOD detectors. However, the exact reasons for the success of NN Guidance are poorly understood. In this work, we take a closer look at NN Guidance and uncover the core reason behind its success - the complementarity between the classifier- and NN-based scores. Put simply, the two scores are complementary when they detect diverse OOD samples, and thus they can perform better when combined. Guided by these insights, we make three main contributions. First, we design a strong baseline OOD detector based on NN Guidance with improved score complementarity. Second, we propose a novel model pruning strategy that further enhances the complementarity and improves performance. Third, we propose a novel method to combine complementary signals from different hidden DNN layers to improve NN Guidance. Finally, by integrating all the sources of complementary information into a unified framework - CoNNGuide - we achieve state-of-the-art performance on CIFAR and ImageNet benchmarks, outperforming prior methods by up to 5.7% in FPR and 2.79% in AUROC.

## 1 INTRODUCTION

Modern machine learning systems are increasingly deployed in open-world settings, where inputs encountered at test time may differ significantly from the training distribution Afshari et al. (2022); Hendrycks et al. (2021). Such out-of-distribution (OOD) inputs can cause models to fail silently, making OOD detection a critical safety requirement in applications like autonomous driving and medical diagnosis Hains et al. (2018); Ren et al. (2021); Zadorozhny et al. (2023). A growing body of research has focused on deriving score functions from neural networks to distinguish in-distribution (ID) from OOD inputs to address this challenge.

The dominant approach to OOD detection involves deriving a scalar score function that captures the “familiarity” of an input—assigning high scores to in-distribution (ID) data and low scores to unfamiliar, OOD examples. Two major families of methods have emerged: classifier-based scores, which use a model’s predictive confidence (e.g., softmax, energy Liu et al. (2020)), and distance-based scores, which assess similarity to training samples in feature space via k-nearest neighbors (KNN) Sun et al. (2022). Classifier-based methods excel at capturing fine-grained differences near decision boundaries, but often fail far from the data manifold. Conversely, distance-based methods are more reliable for far-OOD detection but struggle with near-OOD inputs.

A promising recent direction is nearest-neighbor (NN) guidance, which aims to combine the strengths of classifier- and NN-based scores. One such method, NNGuide Park et al. (2023), computes a unified score that leverages both components. While NNGuide achieves strong empirical

054 performance when paired with certain classifier-based scores, its effectiveness varies widely depending  
 055 on the score it guides—sometimes offering no gain. The factors causing this variance remain  
 056 poorly understood.

057 In this work, we revisit NNGuide from a principled perspective and ask: what exactly enables im-  
 058 proved OOD detection? Our investigation reveals two key factors: The first is the complementarity  
 059 between the classifier-based and nearest-neighbor scores. To put it simply, if the two scores, when  
 060 applied independently, detect diverse OOD examples, then combining them via guidance will give  
 061 a larger improvement. The second factor is the feature space used for nearest neighbor search.  
 062 Different DNN hidden layers produce features with different properties, thus affecting the nearest  
 063 neighbor search and consequently the guidance quality.

064 With access to the above insights, we propose a principled way to build a high-performance OOD  
 065 pipeline using NN guidance. First, we construct a strong baseline OOD detector by combining exist-  
 066 ing improvements to the classifier-based score, and show that higher classifier- and NN-based scores  
 067 complementarity reflects the improved performance. Second, we propose a novel weight pruning  
 068 strategy that improves the robustness of classifier-based scores, leading to improved complementar-  
 069 ity with the NN score and better OOD performance when used with NN guidance. Third, we propose  
 070 multi-guidance - a way to combine multiple NN scores (computed at different DNN layers) into one,  
 071 which further promotes complementarity with classifier-based scores and improves OOD detection.  
 072 Finally, we build the whole pipeline - CoNNGuide (Complementary Nearest Neighbor Guidance) -  
 073 which integrates the complementary contributions of each component and achieves state-of-the-art  
 074 OOD detection performance.

075 To evaluate the performance of CoNNGuide, we perform experiments for OOD detection on three  
 076 popular benchmarks, namely, CIFAR-10, CIFAR-100, and ImageNet with the DenseNetHuang et al.  
 077 (2017), ResNet50 He et al. (2015), and RegNet Xu et al. (2023) models. Our results show that  
 078 CoNNGuide outperforms prior methods by up to 5.7% in false positive rate (FPR) and 2.79% in  
 079 AUROC.

080 In summary, this work makes the following contributions: 1) **A principled framework for analyz-  
 081 ing NN Guidance with score complementarity**, leading to a strong baseline OOD detector com-  
 082 posed of carefully matched classifiers- and NN-based scores. 2) **A novel network pruning strategy  
 083 and new score guidance formulation**, both of which enhance score complementarity and improve  
 084 NN guidance. 3) **A unified OOD detection pipeline, CoNNGuide**, that achieves state-of-the-art  
 085 performance across multiple benchmarks and model architectures.

086 The rest of the paper is organized as follows: Section “Related work” compares CoNNGuide to re-  
 087 lated work. Section “Preliminaries” gives the background material for our work. Section “Our Ap-  
 088 proach” describes our methodology, CoNNGuide, to leverage existing OOD detection approaches to  
 089 filter effectively the unreliable DNN outputs. Section “Experimental results” presents the empirical  
 090 evaluation of the CoNNGuide’s effectiveness and efficiency. Section “Conclusion” concludes the  
 091 paper and discusses future research.

## 094 2 RELATED WORK

097 Out-of-distribution (OOD) detection has emerged as a critical component for building reliable ma-  
 098 chine learning systems. Broadly, prior works can be categorized into two methodological lines:  
 099 classifier-based approaches and distance-based approaches. Classifier-based methods operate on a  
 100 trained model’s output confidence, often using scores such as the maximum softmax probability  
 101 (MSP), energy Hendrycks & Gimpel (2018), or logit-based alternatives like MaxLogit Hendrycks  
 102 et al. (2022) and KL divergence Hendrycks et al. (2022). These approaches are effective at capturing  
 103 uncertainty near decision boundaries but tend to misclassify far-OOD examples overconfidently.

104 Distance-based methods, on the other hand, evaluate the similarity between test inputs and training  
 105 data in feature space. Techniques such as the Mahalanobis distance Lee et al. (2018), SSD Sehwag  
 106 et al. (2021), and KNN-based detection Sun et al. (2022) have shown strong performance in iden-  
 107 tifying far-OOD samples. However, they often lack the fine-grained discriminative capability of  
 classifier-based scores and underperform on near-OOD instances.

To harness the complementary strengths of these paradigms, recent work has explored hybrid methods. NNGuide Park et al. (2023) represents a seminal effort in this direction. It proposes a confidence-guided NN scoring mechanism, where classifier scores are modulated by similarity to nearby training features. This simple, post-hoc mechanism improves both robustness to far-OODs and sensitivity to near-OODs. However, the effectiveness of NNGuide is tightly coupled with the base classifier score and the underlying feature space, and its performance gains vary significantly across settings.

Beyond detection scores, various network truncation and feature rectification techniques such as ReAct Sun et al. (2021), DICE Sun & Li (2022), LINe Ahn et al. (2023), RankFeat Song et al. (2022), and BATS Zhu et al. (2022) have been proposed to enhance the ID-OOD separability. These methods often improve performance when combined with appropriate OOD scores.

### 3 PRELIMINARIES

In this section, we define the problem of OOD detection more formally and revise the details of the NN guidance Park et al. (2023) and importance-based pruning Ahn et al. (2023) approaches.

**Out-of-Distribution (OOD) Detection.** Out-of-distribution (OOD) detection identifies inputs that lie outside the training distribution, which can otherwise cause incorrect or overconfident predictions. A common approach is to compute a scalar OOD score  $S(\mathbf{x})$  that reflects the model’s confidence in a given input  $\mathbf{x}$ . If the score exceeds a threshold  $\lambda$ , the input is considered in-distribution (ID); otherwise, it is deemed out-of-distribution (OOD). This decision rule is formalized as:

$$D(\mathbf{x}) = \begin{cases} \text{ID}, & \text{if } S(\mathbf{x}) \geq \lambda \\ \text{OOD}, & \text{otherwise} \end{cases} \quad (1)$$

Typically, the  $\lambda$  parameter is chosen to be the 95th bottom percentile of the score  $S(\mathbf{x})$  distribution in the training set.

Detection scores can broadly be categorized into two types:

- **Classifier-based scores**, derived from the model’s output logits (e.g., maximum softmax probability Hendrycks et al. (2022), energy-based Liu et al. (2020) scores), leverage class-specific information and are typically effective at detecting near-OOD instances close to decision boundaries.
- **Distance-based scores**, such as k-nearest neighbors (KNN) Sun et al. (2022) or Mahalanobis distance Lee et al. (2018), rely on the similarity between test and training features, and are better suited to detecting far-OOD samples.

**Nearest Neighbor Guidance (NNGUIDE).** NNGuide Park et al. (2023) is a post-hoc, training-free method that combines the strengths of classifier- and distance-based OOD detection. It starts with a base confidence score  $S_{\text{base}}(\mathbf{x})$  - typically classifier-derived - and adjusts it using a nearest-neighbor-based guidance term  $G(\mathbf{x})$ , yielding a final guided score:

$$S_{\text{NNGuide}}(\mathbf{x}) = S_{\text{base}}(\mathbf{x}) \cdot G(\mathbf{x})$$

The guidance term  $G(\mathbf{x})$  is computed from a small “bank” of in-distribution samples. It reflects how similar the test input is to the top- $k$  nearest neighbors in this bank, using cosine similarity weighted by the base confidence of each neighbor. Formally:

$$G(\mathbf{x}) = \frac{1}{k} \sum_{i=1}^k s^{(i)} \cdot \cos(z^{(i)}, z)$$

Here,  $z$  is the normalized feature of  $\mathbf{x}$ ,  $z^{(i)}$  are the top- $k$  neighbors in the training set feature space, and  $s^{(i)} = S_{\text{base}}(\mathbf{x}^{(i)})$  are their base confidences.

This guidance corrects the overconfidence of classifier scores in far-OOD regions and retains their fine-grained sensitivity near ID boundaries. As a result, NNGuide can combine the strengths of classifier- and distance-based approaches and improve detection across both near- and far-OOD regimes, offering robust performance with minimal computational overhead.

162 **Importance-based Pruning.** Activation and weight pruning for OOD detection were first introduced as a part of the LINe method Ahn et al. (2023). It aims to reduce the effect of noisy weights and activations on the classifier-based scores, which helps to improve OOD detection. The approach identifies important neurons by computing class-wise Shapley values, a general tool used in global sensitivity analysis Da Veiga et al. (2021), and selectively retains only the most contributive ones.

163 Given a pre-trained model with penultimate layer activations  $h(x) = [a_1, a_2, \dots, a_d] \in \mathbb{R}^d$  for an  
 164 input  $x$ , where  $d$  is the number of neurons in the penultimate layer, and  $f_\theta(x) = (\mathbf{W}^\top \mathbf{h}(x) + \mathbf{b}) \in$   
 165  $\mathbb{R}^L$  is the class logits of  $L$  classes, LINe estimates the contribution  $s_i^{(l)}$  of neuron  $i$  to class  $l$  using a  
 166 first-order Taylor approximation of the Shapley indices Shapley (1953):  
 167

$$s_i^{(l)} = \left| a_i \cdot \frac{\partial f_\theta(x^{(l)})}{\partial a_i} \right| \quad (2)$$

172 where  $a_i$  is the activation of neuron  $i$ , and  $x^{(l)}$  is an input from class  $l$ . Averaging these values  
 173 over training samples of class  $l$  produces a contribution matrix  $\mathbf{C} \in \mathbb{R}^{d \times L}$ , where each column  
 174 corresponds to a class.

175 For each class  $l$ , the top- $k$  neurons with the highest contributions are selected to form a binary mask  
 176 vector  $\mathbf{m}^{(l)} \in \{0, 1\}^d$ , where ones indicate the retained neurons. To prune the weight matrix, the  
 177 authors select the top- $k$  weight entries according to the contribution matrix  $\mathbf{C}$ . The resulting pruned  
 178 weight matrix  $\hat{\mathbf{W}}$  is then used to obtain the logits. At inference time, given a predicted class  $l$ , the  
 179 activation-pruned model output becomes:  
 180

$$f_{\text{IP}}(x) = \hat{\mathbf{W}}^\top (\mathbf{m}^{(l)} \odot \mathbf{h}(x)) + \mathbf{b} \quad (3)$$

184 where  $\hat{\mathbf{W}} \in \mathbb{R}^{d \times L}$  is the pruned weight matrix,  $\mathbf{b} \in \mathbb{R}^L$  is the bias, and  $\odot$  denotes element-wise  
 185 multiplication. More details about  $\mathbf{C}$ ,  $\hat{\mathbf{W}}$ , and  $\mathbf{m}^{(l)}$  can be found in Ahn et al. (2023).

186 This pruning removes low-contribution neurons that may introduce noise, enabling more robust  
 187 OOD detection by focusing only on class-specific informative features and weights.  
 188

## 191 4 EXPLAINING NNGUIDE’S PERFORMANCE THROUGH SCORE 192 COMPLEMENTARITY

195 In this section, we start by sharing our findings regarding what makes NNGuide work and how to  
 196 use these findings to build a SoTA pipeline for OOD detection.

197 We begin by taking a closer look at NNGuide, which aims to improve OOD detection by combining  
 198 classifier- and distance-based scores. While the original paper reports consistent gains when classi-  
 199 fier scores are guided by a NN-based score, not all classifier scores benefit equally. This variability is  
 200 not addressed in the original work, yet we believe it is central to unlocking NNGuide’s full potential.

201 Our hypothesis is that for NN guidance to be effective, the classifier score must be *complementary*  
 202 to the NN score. That is, each score should be able to detect different OOD examples when applied  
 203 independently (following the decision rule in Equation 1). To test this, we evaluate a range of  
 204 classifier-based scores and measure their complementarity with a NN-based score computed from  
 205 penultimate-layer features, as in Park et al. (2023).

206 We define complementarity as the fraction of OOD examples detected by either method alone:

$$r_{\text{comp}} = \frac{\sum_{i \in S_{\text{OOD}}} (I_{\text{cls}}(i) \vee I_{\text{nn}}(i))}{N_{\text{OOD}}} \quad (4)$$

210 Here,  $I_{\text{cls}}(i)$  and  $I_{\text{nn}}(i)$  are indicator functions that equal 1 if the  $i$ -th OOD example is detected by  
 211 the classifier- or NN-based method, respectively.  $S_{\text{OOD}}$  denotes the set of OOD examples, with a  
 212 total size of  $N_{\text{OOD}}$ .

213 This metric captures the intuition that if either score can detect an OOD sample independently, then  
 214 their combination via NNGuide is likely to detect it as well. In other words, a higher comple-  
 215 mentarity ratio means a better OOD detection performance after applying NNGuide. Moreover, it has

been noticed in computer vision tasks as well that complementary information boosts NN’s performance Dvornik et al. (2019), and we expect similar phenomena to occur in OOD detection. We use the complementarity ratio metric to shed light on why various modifications to the classifier-based score lead to improved OOD detection when used with NN guidance.

**NNGuide++.** We observe that the literature on OOD detection is rich with diverse scoring methods and neural network enhancements—each effective in isolation. In this section, we propose NNGuide++ - a new composite framework, based on NNGuide, with a new, improved classifier-based score. The new classifier score is obtained by carefully integrating multiple OOD detection components, such as the energy score Liu et al. (2020), ReAct Sun et al. (2021), and significance pruning Ahn et al. (2023). We show that the resulting pipeline already achieves new SoTA, and every individual component improves the overall performance. To understand why, we perform analysis through complementary ratios (see Eq 4). More precisely, starting with the energy score as the base classifier score, we add the improvements one at a time, and measure the OOD performance and the complementarity score (with an NN score). The results are shown in Table 1. Crucially, we can see that the improved OOD detection and complementarity are correlated. To verify this claim, we plug in a less capable device MaxLogit Hendrycks et al. (2022) or MSP Hendrycks & Gimpel (2018) into the pipeline and see both the improvement and the complementarity ratio go down, suggesting that the improved performance of the NN guide framework is indeed explained by the classifier- and NN-based score complementarity. The above justifies our choice of individual parts of NNGuide++ and allows for a deeper understanding of further pipeline improvements.

Base scores	Complementarity Ratios (%)	More Complementary?	FPR95 ↓	AUROC ↑	Improvement
Energy Liu et al. (2020)	89.26	-	24.79	94.99	-
MaxLogit Hendrycks & Gimpel (2018)	89.1	x	25.12	94.9	x
MSP Hendrycks et al. (2022)	86.15	x	45.57	93.79	x
ReAct Sun et al. (2021)	89.49	✓	21.21	96.13	✓
ReAct+Shap Ahn et al. (2023)	91.35	✓	13.42	97.4	✓

Table 1: How complementarity ratios relate to NNGuide’s improvement. The first column lists the method added to NNGuide; the second, the complementarity ratio between classifier and NN-based scores; the third, whether this ratio improves over Energy only (“-” meaning not applicable). Columns four and five show OOD performance on CIFAR10, and the last column indicates improvement over Energy. “Shap” denotes activation and weight pruning from Ahn et al. (2023). The OOD score used in ReAct is Energy.

## 5 OUR APPROACH

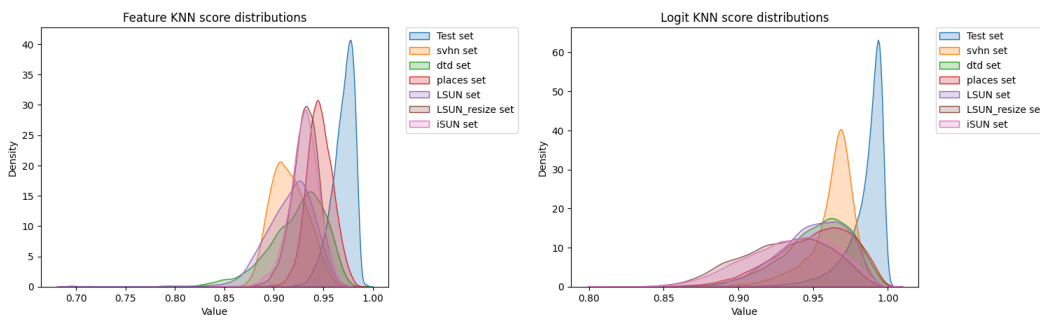
In this section, we present our novel feature pruning strategy and a multi-guidance mechanism that further enhances the framework, which together lead to our complete method - CoNNGuide.

### 5.1 IMPORTANCE-BASED ACTIVATION PRUNING WITH CLASS-PROBABILITY INFORMATION

We focus now on improving the individual components of the pipeline, starting with model pruning based on Shapley indices. Activation pruning in OOD detection aims to improve the classifier score by removing activations that are unimportant for classification and that introduce noise into the score computation Ahn et al. (2023). While the original approach measures each neuron’s contribution to the logits, classification ultimately depends on the softmax probabilities rather than the raw logits. Computing importance solely on per-class logits assumes that class contributions are independent, which can misidentify unimportant neurons that affect all logits equally (and thus do not change class probability) as important. For example, a neuron  $a_i$  may change every logit by the same amount, leaving the class probabilities unchanged and thus irrelevant to the final decision. To address this undesired property, we propose  $P$ -Shapley indices that consider the class probabilities when computing the neuron’s importance. More formally, we change the Equation 2 as follows:

$$s_i^{(l)} = \left| a_i \cdot \frac{\partial (f_\theta(x^{(l)}) \cdot p_\theta(x^{(l)}))}{\partial a_i} \right|, \quad (5)$$

where  $p_\theta(x^{(l)})$  are the class probabilities. By pruning neurons based on their effect on the softmax outputs (and otherwise following Equation 3), we improve the complementarity ratio by 2.22% on CIFAR-10 Krizhevsky (2009), yielding better OOD detection performance.

270 5.2 MULTI-GUIDANCE: EXPLORING COMPLEMENTARITY AMONG HIDDEN LAYERS FOR NN  
271 GUIDANCE  
272273 So far, we have focused on improving the classifier-based score used for guidance. However, we  
274 have largely overlooked the other component of the guidance mechanism—the distance-based score  
275 computed via nearest neighbors (NN). Previous works Park et al. (2023); Lee et al. (2018) that  
276 employ distance-based scores rely exclusively on the penultimate layer of the DNN as the feature  
277 representation for NN search and distance computation.278 However, different layers in a DNN capture varying levels of semantic information, which may  
279 offer complementary signals for OOD detection. For example, Figure 1 shows the distribution of  
280 activations from the last two layers of the pretrained DenseNet on CIFAR10, clearly illustrating the  
281 difference in the encoded information between the ID and OOD data.293 (a) The feature NN guidance score distributions ob- (b) The logit NN guidance score distributions obtained  
294 tained with the pretrained densenet on CIFAR10. with the pretrained densenet on CIFAR10.295 Figure 1: An illustration for the NN guidance scores on different layers using the pretrained  
296 DenseNet model on CIFAR10 dataset.  
297298 To this end, we propose *multi-guidance*—an approach that leverages the complementary information  
299 from different DNN layers to enhance the NNGuide framework. Suppose we aim to use NN scores  
300  $\{G_1, \dots, G_n\}$ , derived from intermediate DNN layers  $\{l_1, \dots, l_n\}$ , to guide the classifier-based  
301 score  $S$ . Each  $G_i$  is computed as the normalized average cosine similarity between its feature vector  
302 ( $z_i$ ) and the ones of its top-k neighbors ( $z_i^{(j)}$ ) in layer  $l_i$ . Then, the multi-guidance score is defined  
303 as:  
304

305 
$$G_i(\mathbf{x}) = \frac{1}{k} \sum_{j=1}^k \frac{1 + \cos(z_i^{(j)}, z_i)}{2}, \quad G_{\text{multi}}^{\overline{1, n-1}} = S \cdot \prod_{i=1}^n G_i = G_{\text{multi}}^{\overline{1, n-1}} \cdot G_n \quad (6)$$

306 In other words, multi-guidance is achieved by replacing the single-layer NN-based score with a  
307 product of NN-based scores from multiple layers, as shown in the first equality.  
308309 A more informative perspective on multi-guidance stems from recognizing that guidance is simply  
310 the operation of multiplying two scores, which do not necessarily need to be a classifier- and a  
311 distance-based score. Thus, multi-guidance can be defined recursively—as expressed by the second  
312 equality in Equation 6—by treating it as NN guidance applied to a score that is itself the result of  
313 prior guidance (originating from different layers’ NN scores).314 This recursive formulation offers deeper insight, as it allows us to analyze multi-guidance using  
315 our complementarity ratio—by computing how complementary  $G_{\text{multi}}^{\overline{1, n-1}}$  and  $G_n$  are. This, in turn,  
316 enables a principled selection of DNN layers that can improve the final detection framework. Going  
317 forward, we refer to multi-guidance as  $G_{\text{multi}}$ , unless we want to specify the used layers explicitly.  
318319 5.3 CONNNGUIDE: PUTTING IT ALL TOGETHER  
320321 We now bring together the components introduced above into a unified OOD detection pipeline:  
322 CoNNNGuide. Given a test input  $\mathbf{x}$ , we first extract intermediate activations from a pre-trained clas-  
323 sifier. These activations are pruned using our P-Shapley (see Eq 5) indices and subsequently used to  
compute the classifier-based score  $S$ .

In parallel, we compute multiple NN-based scores  $\{G_{n-1}, G_n\}$  from the last two (the penultimate and logits) layers. We chose the last two layers because those have low intra-class and high inter-class variance and thus are best suited for OOD detection Masarczyk et al. (2023); Lakshminarayanan et al. (2017). These scores are combined via Equation 6 to form the multi-layer guidance score. Finally, we use the multi-guidance score—i.e.,  $S_{\text{CoNNGuide}} = G_{\text{multi}}$ —to detect OOD examples. This design yields a simple, modular, and highly effective OOD detection system capable of achieving state-of-the-art performance.

## 6 EXPERIMENTAL RESULTS

In this section, we evaluate the performance of our strong baseline NNGuide++, and our complete method, CoNNGuide, and perform the analysis of the novel components.

**Computing resources.** All experiments were performed using the NVIDIA GeForce RTX 4080 Laptop graphics card and the CPU i9-13900HX. When performing GPU-accelerated nearest neighbour (NN) search, it takes up to 10 minutes each, depending on the model and dataset.

**Competitive Methods.** The goal of this work is not only to develop a new OOD detection approach but also to perform a thorough comparison to existing methods. We compare our method CoNNGuide against a comprehensive suite of baseline and state-of-the-art (SoTA) OOD detection techniques, including: MSP Hendrycks & Gimpel (2018), MaxLogit and KL Hendrycks et al. (2022), Energy Liu et al. (2020), ReAct Sun et al. (2021), Mahalanobis Lee et al. (2018), DICE Sun & Li (2022), KNN Sun et al. (2022), NNGuide Park et al. (2023), and LINe Ahn et al. (2023). These methods span both traditional and recent advancements in OOD detection and serve as strong baselines to assess the effectiveness of our approach.

**Evaluation Metrics.** We adopt the standard evaluation metrics commonly used in recent SoTA works Ahn et al. (2023); Sun & Li (2022); Park et al. (2023): (i) the false positive rate at 95% true positive rate (FPR95), and (ii) the area under the receiver operating characteristic curve (AUROC). Unless stated otherwise, all reported values correspond to averages over the relevant OOD datasets used in each experiment.

### 6.1 EVALUATION ON CIFAR BENCHMARKS

**Implementation Details.** We evaluate the proposed methodology on the CIFAR10 and CIFAR100 datasets Krizhevsky (2009), the common OOD detection benchmarks. Their test sets are considered as ID data. We use the same pretrained models in Sun & Li (2022): the DenseNet-101 Huang et al. (2017) being trained for 100 epochs with a learning rate of 0.1, batch size 64, weight decay of 0.0001 and momentum of 0.9. The penultimate layer (i.e., feature vectors) has a size of 342. We also chose the same OOD datasets in Sun & Li (2022) to apply a valid comparison with the competitive methods; these sets are Textures Cimpoi et al. (2014), SVHN Netzer et al. (2011), Places365 Zhou et al. (2017), LSUN-Crop Yu et al. (2016), LSUN-Resize Yu et al. (2016), and iSUNXu et al. (2015). The results are shown in Table 2.

Method	CIFAR-10		CIFAR-100	
	FPR95 ↓	AUROC ↑	FPR95 ↓	AUROC ↑
MSP	48.6	92.52	80.75	73.83
MaxLogit	26.56	94.65	69.78	80.37
KL	26.38	94.76	69.82	80.7
Energy	26.38	94.64	69.84	80.47
ReAct	22.9	95.87	65.42	84.1
Mahalanobis	17.65	95.84	32.73	91.62
DICE	21.7	94.97	51.59	86.54
KNN	16.12	96.8	42.18	87.54
DICE + ReAct	16.11	96.74	44.53	87.2
NNGuide	22.36	95.9	62.16	81.61
LINe	14.7	97.13	31.71	89.21
<b>NNGuide++</b>	<b>13.48</b>	<b>97.4</b>	<b>28.57</b>	<b>90.87</b>
<b>CoNNGuide (Ours)</b>	<b>12.77</b>	<b>97.45</b>	<b>26.01</b>	<b>92</b>

Table 2: OOD detection performance comparison between our methods and the competitive methods on the CIFAR datasets.

378 **SoTA Comparison.** Table 2 demonstrates the comparisons of our methods to existing baselines.  
 379 Significantly, our strong baseline - NNGuide++, already outperforms all the existing methods by  
 380 a sizable margin. More precisely, the strong baseline NNGuide++ surpasses LINE, which has the  
 381 best performance across the existing methods on CIFAR10 and CIFAR100, by 1.22% and 3.14% in  
 382 terms of FPR95 on each dataset. On top of that, our full methods - CoNNGuide - further outperforms  
 383 NNGuide++ by 0.71% and 2.56%, resulting in a total improvement of 1.93% and 5.7%. The same  
 384 observations can be made for AUROC, where CoNNGuide outperforms LINE by 0.32% and 2.79%  
 385 on CIFAR10 and CIFAR100 datasets. These results showed that CoNNGuide had successfully  
 386 surpassed the existing SoTA methods by identifying the important feature (i.e., significant neurons  
 387 in the penultimate layer) more accurately and introducing additional guidance from the logit layer.

## 388 389 6.2 EVALUATION ON IMAGENET

390 **Implementation Details.** The real vision classification is more complicated and possesses more  
 391 target classes. To validate the OOD detection performance of our methodology in real-world sce-  
 392 narios, we evaluate CoNNGuide on the Imagenet-1K dataset Russakovsky et al. (2015), which is a  
 393 large-scale dataset with high-resolution images. Similar to the CIFAR implementation, we utilize  
 394 the test set from Imagenet as our ID data. We considered five OOD datasets: Textures Cimpoi et al.  
 395 (2014), Places365 Zhou et al. (2017), iNaturalist Van Horn et al. (2018), SUN Xiao et al. (2010)  
 396 and OpenImage-OWang et al. (2022), the first four datasets are called “curated datasets” and are  
 397 used for the standard benchmarking on Imagenet. We use two pretrained models for the evalua-  
 398 tion: a ResNet50 He et al. (2016) and a RegNet PyTorch Team (2024), which are both trained on  
 399 Imagenet-1K. The results are displayed in Table 3.

Method	ResNet50		RegNet	
	FPR95 ↓	AUROC ↑	FPR95 ↓	AUROC ↑
MSP	65.08	82.75	45.54	88.27
MaxLogit	58.05	87	28.12	92.29
KL	57.78	87	26.8	92.47
Energy	57.78	87	26.77	92.49
DICE	35.7	90.9	26.77	92.49
Mahalanobis	46.34	90.19	35.32	92.22
KNN	53.53	85.2	25.6	93.08
NNGuide	26.86	92.69	17.97	95.42
LINE	20.7	95.03	26.58	92.5
<b>NNGuide++</b>	<b>17.93</b>	<b>96.1</b>	<b>16.04</b>	<b>96.36</b>
<b>CoNNGuide (Ours)</b>	<b>16.36</b>	<b>96.43</b>	<b>14.85</b>	<b>96.74</b>

412 Table 3: Performance comparison for the curated OOD sets between our methods and the competi-  
 413 tive methods on the Imagenet dataset. The shown **FPR95** and **AUROC** are the average values over  
 414 the considered OOD datasets except OpenImage-O.

415 **SoTA Comparison.** For the ResNet50 model, the built strong baseline NNGuide++ also outper-  
 416 forms the existing SoTA methods directly, and by introducing the Multi-guidance and P-Shapley  
 417 indices, CoNNGuide achieves the state-of-the-art performance by surpassing LINE with an im-  
 418 provement of 4.34% and 1.4% in terms of FPR95 and AUROC. Same for the RegNet model, CoN-  
 419 NGuide outperforms NNGuide, which is the current SoTA for the OOD detection on Imagenet,  
 420 by reducing FPR95 to 14.85% and increasing AUROC to 96.74%. These results demonstrate that  
 421 CoNNGuide possesses a good performance for OOD detection on large-scale and high-resolution  
 422 scenarios, which can be seen as proof of its application in real-world situations.

Method	PShap	MD	FPR95 (Curated) ↓	AUROC (Curated) ↑	FPR95 ↓	AUROC ↑
NNGuide++			17.93	96.1	22.53	94.89
NNGuide++ with PShap	✓		17.55	96.2	22.25	94.87
NNGuide++ with MD		✓	16.48	96.45	21.89	95.1
CoNNGuide (Ours)	✓	✓	16.36	96.43	21.68	95.12

428 Table 4: Ablation study on the proposed novel techniques with the pretrained ResNet50 on Imagenet.  
 429 **FPR95 (Curated)** and **AUROC (Curated)** are the average values over the chosen OOD datasets  
 430 except OpenImage-O. **FPR95** and **AUROC** are the average values over all the OOD datasets.

Method	PShap	MD	FPR95 ↓	AUROC ↑
NNGuide++			28.58	90.87
NNGuide++ with PShap	✓		28.49	91.05
NNGuide++ with MD		✓	26.22	91.8
CoNNGuide (Ours)	✓	✓	26.01	92

Table 5: Ablation study on the proposed techniques with the pretrained DenseNet on CIFAR100.

### 6.3 ANALYSIS

The goal of this section is to evaluate individual contributions and analyze the complementarity properties of the novel components of CoNNGuide introduced in this paper.

**Ablation Study.** We analyze the individual components by performing ablations on (i) the P-Shapley indices used to prune the activation and weights of the network, and (ii) the multi-guidance approach, gathering information from multiple DNN layers to improve OOD detection. Since both components are built on top of our strong baseline, NNGuide++, we chose it as the baseline here.

Table 5 and 4 show the ablation study for the main CoNNGuide’s components. The results in both tables show that each novel component improved the OOD detection performance. More precisely, for the Imagenet dataset, introducing the P-Shapley indices for activation importance identification reduces FPR95 by 0.38% and the NN guidance through logit information improves FPR95 by 1.45%. With both techniques, we successfully reduce FPR95 to 16.36%. Similarly, for the CIFAR100 dataset, the P-Shapley indices and the logit NN guidance reduce FPR95 by 2.57% compared to the proposed strong baseline NNGuide++, and improve the AUROC by 1.13%.

Base scores	Complementarity Ratios (%)	FPR95 ↓	AUROC ↑
Energy	89.26	24.79	94.99
ReAct	89.49	21.21	96.13
ReAct+PShap	91.71	13.32	97.44
ReAct+PShap+MD	91.92	12.77	97.45

Table 6: Complementarity ratios and performance after the feature guidance for the detected OOD examples with the feature NN scores and different base scores on CIFAR10 dataset. PShap stand for P-Shapley and MD is Multi-guidance. The OOD score used in ReAct is Energy.

**Complementarity of CoNNGuide Components.** Here, we measure the complementarity properties of the components of CoNNGuide. To do so, we build up the CoNNGuide pipeline, starting from vanilla Energy scoreLiu et al. (2020), and measure the complementarity of the classification- and NN-based scores on CIFAR10. As shown in Table 6, both the selection of important neurons based on P-Shapley indices and Multi-guidance improve the complementarity score and lead to the improved final performance of CoNNGuide.

## 7 CONCLUSION

In this work, we revisited the problem of OOD detection through the lens of nearest-neighbor guidance. We introduced a principled framework for understanding and exploiting the complementarity of OOD detection scores. By carefully analyzing the conditions under which classifier-based and distance-based scores synergize, we proposed a systematic method to construct strong baselines from existing components. We further enhanced this foundation with two novel contributions: P-Shapley pruning, which improves the robustness and complementarity of classifier-based scores, and multi-guidance, which aggregates signals across multiple feature layers. These insights culminated in CoNNGuide, a simple yet highly effective detection pipeline that achieves state-of-the-art results across CIFAR and ImageNet benchmarks. It must be noted that our method inherits the limitations of NNGuide, and, for example, is expected to benefit from combining multiple NN-based scores to a lesser degree. Nevertheless, our findings highlight the central role of complementarity in guided OOD detection and offer the potential to build upon this work in future research.

486 REFERENCES  
487

488 Sajad Saraygord Afshari, Fatemeh Enayatollahi, Xiangyang Xu, and Xihui Liang. Machine  
489 learning-based methods in structural reliability analysis: A review. *Reliab. Eng. Syst. Saf.*, 219:  
490 108223, 2022. doi: 10.1016/J.RESS.2021.108223.

491 Yong Hyun Ahn, Gyeong-Moon Park, and Seong Tae Kim. Line: Out-of-distribution detection by  
492 leveraging important neurons. In *2023 IEEE/CVF Conference on Computer Vision and Pattern  
493 Recognition (CVPR)*, pp. 19852–19862, 2023. doi: 10.1109/CVPR52729.2023.01901.

494

495 Mircea Cimpoi, Subhransu Maji, Iasonas Kokkinos, Sammy Mohamed, and Andrea Vedaldi. De-  
496 scribing textures in the wild. In *2014 IEEE Conference on Computer Vision and Pattern Recog-  
497 nition*, pp. 3606–3613, 2014. doi: 10.1109/CVPR.2014.461.

498

499 Sébastien Da Veiga, Fabrice Gamboa, Bertrand Iooss, and Clémentine Prieur. *Basics and trends in  
500 sensitivity analysis: Theory and practice in R*. SIAM, 2021.

501

502 Nikita Dvornik, Cordelia Schmid, and Julien Mairal. Diversity with cooperation: Ensemble methods  
503 for few-shot classification. In *Proceedings of the IEEE/CVF international conference on computer  
504 vision*, pp. 3723–3731, 2019.

505

506 Gaétan Hains, Arvid Jakobsson, and Youry Khmelevsky. Towards formal methods and software  
507 engineering for deep learning: Security, safety and productivity for dl systems development. In  
508 *Proceedings of the International Systems Conference, SysCon 2018, Vancouver, BC, Canada,  
2018*, pp. 1–5. IEEE, 2018. doi: 10.1109/SYSCON.2018.8369576.

509

510 Kaiming He, Xiangyu Zhang, Shaoqing Ren, and Jian Sun. Deep residual learning for image recog-  
511 nition. *CoRR*, abs/1512.03385, 2015. URL <http://arxiv.org/abs/1512.03385>.

512

513 Kaiming He, Xiangyu Zhang, Shaoqing Ren, and Jian Sun. Identity mappings in deep residual  
514 networks. In Bastian Leibe, Jiri Matas, Nicu Sebe, and Max Welling (eds.), *Computer Vision  
– ECCV 2016*, pp. 630–645, Cham, 2016. Springer International Publishing. ISBN 978-3-319-  
515 46493-0.

516

517 Dan Hendrycks and Kevin Gimpel. A baseline for detecting misclassified and out-of-distribution  
518 examples in neural networks, 2018. URL <https://arxiv.org/abs/1610.02136>.

519

520 Dan Hendrycks, Kevin Zhao, Steven Basart, Jacob Steinhardt, and Dawn Song. Natural adversarial  
521 examples. In *2021 IEEE/CVF Conference on Computer Vision and Pattern Recognition (CVPR)*,  
522 pp. 15257–15266, 2021. doi: 10.1109/CVPR46437.2021.01501.

523

524 Dan Hendrycks, Steven Basart, Mantas Mazeika, Andy Zou, Joseph Kwon, Mohammadreza Mosta-  
525 jabi, Jacob Steinhardt, and Dawn Song. Scaling out-of-distribution detection for real-world set-  
526 tings. In Kamalika Chaudhuri, Stefanie Jegelka, Le Song, Csaba Szepesvari, Gang Niu, and Sivan  
527 Sabato (eds.), *Proceedings of the 39th International Conference on Machine Learning*, volume  
528 162 of *Proceedings of Machine Learning Research*, pp. 8759–8773. PMLR, 17–23 Jul 2022. URL  
529 <https://proceedings.mlr.press/v162/hendrycks22a.html>.

530

531 Gao Huang, Zhuang Liu, Laurens van der Maaten, and Kilian Q. Weinberger. Densely connected  
532 convolutional networks. In *Proceedings of the IEEE Conference on Computer Vision and Pattern  
533 Recognition (CVPR)*, July 2017.

534

535 Alex Krizhevsky. Learning multiple layers of features from tiny images. pp. 32–33, 2009. URL  
<https://www.cs.toronto.edu/~kriz/learning-features-2009-TR.pdf>.

536

537 Balaji Lakshminarayanan, Alexander Pritzel, and Charles Blundell. Simple and scal-  
538 able predictive uncertainty estimation using deep ensembles. In *Advances in Neu-  
539 ral Information Processing Systems*, volume 30. Curran Associates, Inc., 2017. URL  
[https://proceedings.neurips.cc/paper\\_files/paper/2017/file/9ef2ed4b7fd2c810847ffa5fa85bce38-Paper.pdf](https://proceedings.neurips.cc/paper_files/paper/2017/file/9ef2ed4b7fd2c810847ffa5fa85bce38-Paper.pdf).

540 Kimin Lee, Kibok Lee, Honglak Lee, and Jinwoo Shin. A simple unified frame-  
 541 work for detecting out-of-distribution samples and adversarial attacks. In S. Bengio,  
 542 H. Wallach, H. Larochelle, K. Grauman, N. Cesa-Bianchi, and R. Garnett (eds.), *Ad-*  
 543 *vances in Neural Information Processing Systems*, volume 31. Curran Associates, Inc.,  
 544 2018. URL [https://proceedings.neurips.cc/paper\\_files/paper/2018/file/abdeb6f575ac5c6676b747bca8d09cc2-Paper.pdf](https://proceedings.neurips.cc/paper_files/paper/2018/file/abdeb6f575ac5c6676b747bca8d09cc2-Paper.pdf).

545 Weitang Liu, Xiaoyun Wang, John Owens, and Yixuan Li. Energy-based out-of-distribution  
 546 detection. In *Advances in Neural Information Processing Systems (NeurIPS)*, pp. 21464–  
 547 21475, 2020. URL [https://proceedings.neurips.cc/paper\\_files/paper/2020/file/f5496252609c43eb8a3d147ab9b9c006-Paper.pdf](https://proceedings.neurips.cc/paper_files/paper/2020/file/f5496252609c43eb8a3d147ab9b9c006-Paper.pdf).

548 Wojciech Masarczyk, Mateusz Ostaszewski, Ehsan Imani, Razvan Pascanu, Piotr Miłoś, and  
 549 Tomasz Trzcinski. The tunnel effect: Building data representations in deep neural networks.  
 550 In *Thirty-seventh Conference on Neural Information Processing Systems*, 2023. URL <https://openreview.net/forum?id=xQOHOpelFv>.

551 Yuval Netzer, Tao Wang, Adam Coates, Alessandro Bissacco, Bo Wu, and Andrew Y. Ng. Reading  
 552 digits in natural images with unsupervised feature learning. In *NIPS Workshop on Deep Learning*  
 553 and *Unsupervised Feature Learning 2011*, 2011. URL [http://ufldl.stanford.edu/housenumbers/nips2011\\_housenumbers.pdf](http://ufldl.stanford.edu/housenumbers/nips2011_housenumbers.pdf).

554 Jaewoo Park, Yoon Gyo Jung, and Andrew Beng Jin Teoh. Nearest neighbor guidance for out-of-  
 555 distribution detection. In *Proceedings of the IEEE/CVF International Conference on Computer*  
 556 *Vision (ICCV)*, pp. 1686–1695, October 2023.

557 PyTorch Team. `torchvision.models.regnet_y_16gf`, 2024. URL [https://docs.pytorch.org/vision/main/models/generated/torchvision.models.regnet\\_y\\_16gf.html](https://docs.pytorch.org/vision/main/models/generated/torchvision.models.regnet_y_16gf.html). Accessed: 2025-05-15.

558 Xuanchi Ren, Tao Yang, Li Erran Li, Alexandre Alahi, and Qifeng Chen. Safety-aware Motion  
 559 Prediction with Unseen Vehicles for Autonomous Driving . In *2021 IEEE/CVF International*  
 560 *Conference on Computer Vision (ICCV)*, pp. 15711–15720, Los Alamitos, CA, USA, October  
 561 2021. IEEE Computer Society. doi: 10.1109/ICCV48922.2021.01544. URL <https://doi.ieee.org/10.1109/ICCV48922.2021.01544>.

562 Olga Russakovsky, Jia Deng, Hao Su, Jonathan Krause, Sanjeev Satheesh, Sean Ma, Zhiheng  
 563 Huang, Andrej Karpathy, Aditya Khosla, Michael Bernstein, Alexander C. Berg, and Li Fei-Fei.  
 564 ImageNet Large Scale Visual Recognition Challenge. *International Journal of Computer Vision (IJCV)*, 115(3):211–252, 2015. doi: 10.1007/s11263-015-0816-y.

565 Vikash Sehwag, Mung Chiang, and Prateek Mittal. Ssd: A unified framework for self-supervised  
 566 outlier detection, 2021. URL <https://arxiv.org/abs/2103.12051>.

567 Lloyd S Shapley. A value for n-person games. In Harold W. Kuhn and Albert W. Tucker (eds.),  
 568 *Contributions to the Theory of Games II*, pp. 307–317. Princeton University Press, Princeton,  
 569 1953.

570 Yue Song, Nicu Sebe, and Wei Wang. Rankfeat: Rank-1 feature removal for out-of-distribution de-  
 571 tection. In S. Koyejo, S. Mohamed, A. Agarwal, D. Belgrave, K. Cho, and A. Oh (eds.), *Advances*  
 572 *in Neural Information Processing Systems*, volume 35, pp. 17885–17898. Curran Associates, Inc.,  
 573 2022. URL [https://proceedings.neurips.cc/paper\\_files/paper/2022/file/71c9eb0913e6c7fda3afd69c914b1a0c-Paper-Conference.pdf](https://proceedings.neurips.cc/paper_files/paper/2022/file/71c9eb0913e6c7fda3afd69c914b1a0c-Paper-Conference.pdf).

574 Yiyou Sun and Yixuan Li. Dice: Leveraging sparsification for out-of-distribution detection. In  
 575 *Computer Vision – ECCV 2022: 17th European Conference, Tel Aviv, Israel, October 23–27,*  
 576 *2022, Proceedings, Part XXIV*, pp. 691–708, Berlin, Heidelberg, 2022. Springer-Verlag. ISBN  
 577 978-3-031-20052-6. doi: 10.1007/978-3-031-20053-3\_40. URL [https://doi.org/10.1007/978-3-031-20053-3\\_40](https://doi.org/10.1007/978-3-031-20053-3_40).

578 Yiyou Sun, Chuan Guo, and Yixuan Li. React: Out-of-distribution detection with rectified ac-  
 579 tivations. In *Advances in Neural Information Processing Systems*, 2021. URL [https://openreview.net/forum?id=IBVBtz\\_sRSm](https://openreview.net/forum?id=IBVBtz_sRSm).

594 Yiyou Sun, Yifei Ming, Xiaojin Zhu, and Yixuan Li. Out-of-distribution detection with deep nearest  
 595 neighbors. In *International Conference on Machine Learning*, pp. 20827–20840. PMLR, 2022.  
 596

597 Grant Van Horn, Oisin Mac Aodha, Yang Song, Yin Cui, Chen Sun, Alex Shepard, Hartwig Adam,  
 598 Pietro Perona, and Serge Belongie. The inaturalist species classification and detection dataset. In  
 599 *Proceedings of the IEEE Conference on Computer Vision and Pattern Recognition (CVPR)*, June  
 600 2018.

601 Haodi Wang, Zhizhong Li, Litong Feng, and Wayne Zhang. Vim: Out-of-distribution with virtual-  
 602 logit matching. In *2022 IEEE/CVF Conference on Computer Vision and Pattern Recognition  
 603 (CVPR)*, pp. 4911–4920, 2022. doi: 10.1109/CVPR52688.2022.00487.

604 Jianxiong Xiao, James Hays, Krista A. Ehinger, Aude Oliva, and Antonio Torralba. Sun database:  
 605 Large-scale scene recognition from abbey to zoo. In *2010 IEEE Computer Society Conference  
 606 on Computer Vision and Pattern Recognition*, pp. 3485–3492, 2010. doi: 10.1109/CVPR.2010.  
 607 5539970.

608 Jing Xu, Yu Pan, Xinglin Pan, Steven Hoi, Zhang Yi, and Zenglin Xu. Regnet: Self-regulated  
 609 network for image classification. *IEEE Transactions on Neural Networks and Learning Systems*,  
 610 34(11):9562–9567, 2023. doi: 10.1109/TNNLS.2022.3158966.

612 Pingmei Xu, Krista A Ehinger, Yinda Zhang, Adam Finkelstein, Sanjeev R. Kulkarni, and Jianx-  
 613 iong Xiao. Turkergaze: Crowdsourcing saliency with webcam based eye tracking, 2015. URL  
 614 <https://arxiv.org/abs/1504.06755>.

615 Fisher Yu, Ari Seff, Yinda Zhang, Shuran Song, Thomas Funkhouser, and Jianxiong Xiao. Lsun:  
 616 Construction of a large-scale image dataset using deep learning with humans in the loop, 2016.  
 617 URL <https://arxiv.org/abs/1506.03365>.

619 Karina Zadorozhny, Patrick Thoral, Paul Elbers, and Giovanni Cinà. *Out-of-Distribution Detection  
 620 for Medical Applications: Guidelines for Practical Evaluation*, pp. 137–153. Springer Interna-  
 621 tional Publishing, Cham, 2023. ISBN 978-3-031-14771-5. doi: 10.1007/978-3-031-14771-5\_10.  
 622 URL [https://doi.org/10.1007/978-3-031-14771-5\\_10](https://doi.org/10.1007/978-3-031-14771-5_10).

623 Bolei Zhou, Agata Lapedriza, Aditya Khosla, Aude Oliva, and Antonio Torralba. Places: A 10 mil-  
 624 lion image database for scene recognition. *IEEE Transactions on Pattern Analysis and Machine  
 625 Intelligence*, 2017.

627 Yao Zhu, YueFeng Chen, Chuanlong Xie, Xiaodan Li, Rong Zhang, Hui Xue', Xiang Tian, bolun  
 628 zheng, and Yaowu Chen. Boosting out-of-distribution detection with typical features. In  
 629 S. Koyejo, S. Mohamed, A. Agarwal, D. Belgrave, K. Cho, and A. Oh (eds.), *Advances in  
 630 Neural Information Processing Systems*, volume 35, pp. 20758–20769. Curran Associates, Inc.,  
 631 2022. URL [https://proceedings.neurips.cc/paper\\_files/paper/2022/file/82b0c1b954b6ef9f3cfb664a82b201bb-Paper-Conference.pdf](https://proceedings.neurips.cc/paper_files/paper/2022/file/82b0c1b954b6ef9f3cfb664a82b201bb-Paper-Conference.pdf).

633  
 634  
 635  
 636  
 637  
 638  
 639  
 640  
 641  
 642  
 643  
 644  
 645  
 646  
 647